

See discussions, stats, and author profiles for this publication at: <https://www.researchgate.net/publication/231231231>

Structural Study of Salicylic Acid Salts of a Series of Azacycles and Azacrown Etherst

ARTICLE *in* CRYSTAL GROWTH & DESIGN · OCTOBER 2010

Impact Factor: 4.89 · DOI: 10.1021/cg101002x

CITATIONS

13

READS

54

6 AUTHORS, INCLUDING:



Marina S Fonari

Institute of Applied Physics Academy of Scie...

149 PUBLICATIONS 738 CITATIONS

[SEE PROFILE](#)



Eduard V. Ganin

Odessa State Environmental University

197 PUBLICATIONS 622 CITATIONS

[SEE PROFILE](#)



Konstantin A Lyssenko

Russian Academy of Sciences

761 PUBLICATIONS 6,128 CITATIONS

[SEE PROFILE](#)

Structural Study of Salicylic Acid Salts of a Series of Azacycles and Azacrown Ethers[†]

Marina S. Fonari,^{*‡} Eduard V. Ganin,[§] Stepan S. Basok,^{||} Konstantin A. Lyssenko,[⊥]
Michael J. Zaworotko,[#] and Victor Ch. Kravtsov[‡]

[‡]Institute of Applied Physics, Academy of Sciences of Moldova, Academiei Street, 5 MD-2028 Chișinău, R, Moldova, [§]Odessa State Environmental University, Lvovskaya Strasse 15, 65016 Odessa, Ukraine, ^{||}A. V. Bogatsky Physico-Chemical Institute, National Academy of Sciences of Ukraine, Lustdorfskaya doroga 86, 650080 Odessa, Ukraine, [⊥]A.N. Nesmeyanov Institute of Organoelement Compounds, Russian Academy of Sciences, 28 Vavilov Street B-334, 119991 Moscow, Russia, and [#]Department of Chemistry, University of South Florida, CHE205, 4202 East Fowler Avenue, Tampa, Florida 33620, United States

Received July 30, 2010; Revised Manuscript Received September 23, 2010

ABSTRACT: Interaction of salicylic acid (**saH**) with the azacycles piperidine (**pipe**) and *meso*-5,7,7,12,12,14-hexamethyl-1,4,8,11-tetraazacyclotetradecane (**teta**) and with the aza-crown ethers aza-12-crown-4 (**A12C4**), benzoaza-15-crown-5 (**BA15C5**), aza-18-crown-6 (**A18C6**), and diaza-18-crown-6 (**DA18C6**) afforded the proton-transfer complexes (organic salts) of compositions **[pipeH][sa]**, **[tetaH₂][sa]₂**, **[A12C4H][sa]**, **[BA15C5H][sa]**, **[A18C6H][sa]·2H₂O**, and **[DA18C6H₂][sa]₂·3H₂O**, whose structures were determined by a single crystal X-ray method. These products were also obtained by the same synthetic conditions starting from acetylsalicylic acid (aspirin) as a result of hydrolysis. The charge-assisted N—H···O hydrogen-bond provides the main driving force for direct binding of **sa** with cyclic azonia cations. The crystal packing is also supported by weak C—H···O hydrogen bonding and edge-to-face π···π intermolecular interactions.

The crystal engineering of multicomponent systems including active pharmaceutical ingredients (APIs) has attracted much attention in recent years because the physicochemical properties of the APIs can be changed, thereby altering their pharmaceutical profile. Particularly relevant in this context is aqueous solubility, which can critically influence the ADMET (absorption, distribution, metabolism, excretion, and toxicity) properties of the APIs. Lipophilicity is another key parameter that influences ADMET properties, as only APIs with the appropriate lipophilicity can cross the blood brain barrier for uptake by the brain. Modern strategies to affect these parameters typically focus on salt and cocrystal formation or medicinal chemistry approaches that rely on covalent transformations of the API.¹ Organic acids, especially carboxylic acids, represent ca. 30% of APIs, and they are also widely used as salt or cocrystal formers.^{2,3} We have recently reported five crystal structures formed by reacting *p*-aminobenzoic acid, which is topically used as a sunscreen agent in various pharmaceutical preparations, with azacycles and aza-crown ethers.⁴ We have also reported the crystal structures of four proton-transfer complexes of mefenamic acid, a poorly soluble anti-inflammatory agent, with aza-cycles of different dimensionality.⁵ Our aim was to study the supramolecular synthons that occur between the cation and anion and to determine the contribution of weak interactions to the overall crystal packing. We report herein a new investigation along these lines by reporting how other aromatic pharmaceutical acids react with aza-cycles and crown ethers, thereby offering a new opportunity to study how both strong and weak hydrogen bonding interactions as well as aromatic stacking interactions influence

the crystal packing of APIs. Salicylic acid (2-hydroxybenzoic acid, **saH**) represents an attractive target for this purpose. Salicylic acid, a key ingredient of skin-care products, has antiseptic, preservative, analgesic, and anti-inflammatory properties, covering a broad spectrum of applications,⁶ and it also has some similarities with aspirin, both in its analgesic action and in its crystal packing arrangement⁷ (the formation of a centrosymmetric $R_2^2(8)$ carboxylic acid dimer supramolecular homosynthon occurs both in aspirin polymorphs and in the reported crystal form of salicylic acid⁸). The planar dimers of **saH** are packed into a herringbone motif *via* interactions between *p*-H atoms and hydroxyl groups.⁹ As with most APIs, **saH** is likely to be similar to other APIs in that it should be amenable to formation of cocrystals or salts¹⁰ and form multiple stoichiometry variants of salts and cocrystals,¹¹ and depending upon which method of preparation is employed, there also exist the possibilities of solvates, hydrates, and polymorphic forms. Indeed, the reproducibility of the reaction products is unlikely to be consistent over “routine” solvent crystallization, mechanochemical approaches,¹² and melt crystallization *via* the Kofler mixed fusion method.¹³ Along with the study of crystalline multicomponent compounds, the use of ionic liquids formed between pharmaceutically active ions and pharmaceutically acceptable counterions has recently been suggested by Rogers and co-workers. The salicylate anion has been used in this context.¹⁴ Salicylic acid has already been shown to exist as either a cocrystal former or an anion in multicomponent crystals within the cocrystal-salt continuum.¹⁵ In the commentary by Haynes and co-workers¹⁶ based on the CSD statistics (ConQuest¹⁷ version 1.6 on version 5.25 of the CSD¹⁸), salicylic acid is cited as a component of 19 salts, 7 neutral cocrystals, 1 ionic cocrystal, and 3 cocrystals of salts. This list has since been augmented by salicylic acid and DABCO, phenazine, diacetylpirperazine,¹⁰ 3,5-dimethyl-1H-pyrazole,¹¹

[†]Dedicated to the memory of Yurii A. Simonov.

*To whom correspondence should be addressed. E-mail: fonari.xray@phys.asm.md (M.S.F); and kravtsov.xray@phys.asm.md (V.Ch.K).

Table 1. Selected Structural Data for Salicylic Acid Complexes

guest	SpGr ^a	guest/saH/solvent ^b	CSD code	ref
salicylic acid	<i>P</i> 2 ₁ / <i>a</i>		SALIAC SALIAC01 SALIAC03 SALIAC12 SALIAC15 SALIAC16	9
ammonia	<i>P</i> 2 ₁ / <i>n</i>	1:1 salt	HUCPOL	21
antipyrine	<i>P</i> 2 ₁ / <i>c</i>	1:1 cocrystal	APYSAL	22
piperazine	<i>P</i> 2 ₁ / <i>n</i>	1:2 salt	BAKYES	23
2-amino-3,5-dibromo- <i>N</i> -cyclohexyl- <i>N</i> -methylbenzenemethanamine	<i>P</i> 1 C2/ <i>c</i>	1:1 salt	BUSNIM BUSNIM10	24, 25
2-amino-4,6-dimethoxypyrimidine	<i>P</i> 2 ₁ / <i>c</i>	1:1 salt	CIQBIO	26
creatinine	<i>P</i> 2 ₁ / <i>n</i>	1:1 salt	DENXAW	27
β -cyclodextrin, acetylsalicylic acid	<i>P</i> 1	2:2:1:23.3 (H ₂ O) clathrate	DIFHOP	28
piperazine-2,5-dione	<i>P</i> 2 ₁ / <i>a</i>	1:2 cocrystal	DKPSAL10	29
5-fluorocytosine	<i>P</i> 2 ₁ / <i>n</i>	1:1 salt	EDATOS	30
<i>N</i> -carboxymethyl- <i>N</i> -methylmorpholine	<i>P</i> bca	1:1 salt	EMUREJ	31
tetra- <i>n</i> -butylamine thiourea	<i>P</i> 1	1:1:1:0.5 (H ₂ O) cocrystal of salt	FIXTAI	32
sulfadimidine	<i>P</i> bca	1:1 cocrystal	GEYSAE	33
tetradecyltrimethylamine	<i>P</i> 1	1:1:1 (H ₂ O) salt	HABVIP	34
hexadecyltrimethylamine	<i>P</i> 1	1:1:1 (H ₂ O) salt	HABVOV	34
8-hydroxyquinoline	<i>P</i> 2 ₁	1:1 salt	HURNEN	35
1,12,15-triaza-3,4:9,10-bis(4'- <i>tert</i> -butylbenzo)-5,8-dioxacycloheptadecane	<i>P</i> 2 ₁ / <i>c</i>	1:2:1 (H ₂ O) salt	KAFSEQ	36
theophylline	<i>P</i> 2 ₁ / <i>n</i>	1:1 cocrystal	KIGLES	15b
2-aminopyrimidine	<i>P</i> bca	1:1 salt	LEWROU	37
adenine	<i>P</i> 2 ₁ / <i>n</i>	1:1:1 (CH ₃ OH) salt	LOLDIA	38
physostigmine	<i>P</i> 2 ₁ 2 ₁ 2 ₁	1:1 salt	LUDDUJ	39
trimethoprim	<i>P</i> 1	1:1:1 (CH ₃ OH) salt	MIFWUT	40
nicotine	<i>P</i> 2 ₁	1:1 salt	NICSAL	41
8-hydroxyquinoline	<i>P</i> 1	1:2 cocrystal of salt	NIMDIW	42
3,5-dimethyl-1 <i>H</i> -pyrazole	<i>P</i> na2 ₁	1:2 cocrystal	ODOHEV	11
3,5-dimethyl-1 <i>H</i> -pyrazole	<i>P</i> 2 ₁ / <i>c</i>	2:1 cocrystal	ODOHIZ	11
deoxycholic acid	<i>P</i> 2 ₁ 2 ₁ 2 ₁	1:1 cocrystal	RAVVUF	43
cytidine	<i>P</i> 1	1:1 cocrystal	SALCYS	44
9-methyladenine	<i>P</i> bcn	1:1 salt	SLCADDA10	45
2-aminopyridine	<i>P</i> bca	1:1 salt	SLCADB10	46
urea	<i>C</i> 2/ <i>c</i>	1:1 cocrystal	SLCADC10	45
nicotinamide	<i>P</i> 2 ₁ / <i>n</i>	1:1 cocrystal	SODDOF	13, 15c
quinine	<i>P</i> 2 ₁ 2 ₁ 2 ₁	1:1:1 (H ₂ O) salt	WANTOU	47
2-amino-4,6-dimethylpyrimidine	<i>P</i> 2 ₁	1:1 salt	WEPTIV	48
guanidine	<i>P</i> bca	1:1 salt	XAGFAM	49
isonicotinamide	<i>P</i> 2 ₁ / <i>c</i>	1:1 cocrystal	XAQQEM	50
caffeine	<i>P</i> 2 ₁ / <i>n</i>	1:1 cocrystal	XOBCAT XOBCAT01	19, 12
2',6'-dimethylpiperidine	<i>P</i> 2 ₁ 2 ₁ 2 ₁	1:1 salt	YAVRAO	51
mestanolone	<i>P</i> 2 ₁ 2 ₁ 2 ₁	1:1 cocrystal	YOFWIA	52
carbamazepine	<i>P</i> 2 ₁ / <i>n</i>	1:1 cocrystal	MOXWAY	20
9 <i>H</i> -purin-6-amine	<i>P</i> 2 ₁ / <i>c</i>	1:3 cocrystal	MUBRAD	53
piperidine-3-carboxylic acid	<i>P</i> bca	1:1 cocrystal	YORJOF	54
DABCO	<i>P</i> ccn	1:2 salt	NUKWUM	10
phenazine	<i>P</i> 2 ₁ / <i>c</i>	1:2 cocrystal	NUKXAT	10
<i>N,N'</i> -diacetyl piperazine	<i>P</i> bca, <i>P</i> 1	1:2 cocrystal	NUKXEX NUKXEX01	10
4-aminoantipyrene	<i>P</i> 2 ₁ / <i>c</i>	1:1 salt	DUHYOV	55
gabapentin	<i>P</i> 2 ₁ / <i>n</i>	1:1 salt	FOXPAK	56
piperidine	<i>P</i> 2 ₁ / <i>c</i>	1:1 salt		this work
<i>meso</i> -5,7,7,12,12,14-hexamethyl-1,4,8,11-tetraazacyclotetradecane (teta)	<i>P</i> 2 ₁ / <i>c</i>	1:2 salt		this work
aza-12-crown-4	<i>P</i> 2 ₁ / <i>c</i>	1:1 salt		this work
benzoaza-15-crown-5	<i>P</i> 1	1:1 salt		this work
aza-18-crown-6	<i>P</i> ca2 ₁	1:1:2 (H ₂ O) salt		this work
1,10-diaza-18-crown-6	<i>P</i> 1	1:2:3 (H ₂ O) salt		this work

^a SpGr space group. ^b Assigned based on CSD structures. Only metal free structures with fractional atomic coordinates are included.

caffeine,^{12,19} and carbamazepine.²⁰ In this contribution we present details on the synthesis and structures of a new series of multiple component crystals that include salicylic acid and discuss them in the context of a CSD analysis (version 5.31, release November 2009, including February and May 2010 updates). Table 1 presents a full list of compounds involving salicylic acid as a cocrystal former or counterion.

Crown ethers represent a class of compounds that are exceptionally versatile in that they can selectively bind a range of metal ions and a variety of organic neutral and ionic species.⁵⁷ Our long-term involvement in the crystal chemistry of crown ethers⁵⁸ explains our choice of crown ethers and

aza-cycles as cocrystal formers or counterions. Structurally, when crown ethers are in their “crown” conformation, they possess a hydrophobic ring surrounding a hydrophilic cavity, which enables them to form stable complexes with metal ions and at the same time to be incorporated in the lipid fraction of the cell membrane. Aza-crowns have complexation properties that are intermediate between those of all-oxygen crown ethers, which complex strongly with alkali, alkaline earth, and primary ammonium cations, and those of all-nitrogen cyclams, which complex strongly with the transition metal and heavy metal cations. Contrary to the cases of azacycles (mainly cyclen and cyclam derivatives), which are widely

studied and explored in medicinal chemistry,⁵⁹ the toxicity of crown ethers has limited their study to anticancer agents. In this context, recent studies demonstrate that crown compounds could either induce toxicities that are different from those of conventional antitumor drugs or complement drugs in current use.⁶⁰ Our present study demonstrates the possibility to develop further multicomponent crystalline solids from such macrocycles and thereby modify their physicochemical properties. The aza-cycles and aza-crown ethers studied herein represent a variety of sizes and number of *N*-basic centers, and they are illustrated in Scheme 1.

In solution, ΔpK_a is a useful measure of determining the outcome of an acid–base reaction, since salt formation is expected to happen when ΔpK_a is greater than 2 or 3.¹⁵ In light of the relative strength of salicylic acid ($pK_a = 2.97$) and high pK_a values for the bases in Scheme 1 (they all fall in the range 8.2–12.6),⁶¹ we expect proton transfer to form proton-transfer complexes⁶² or organic salts. Depending on the number and relative arrangement of nitrogen atoms within the molecule, the cyclic bases studied herein were expected to form with **saH** either of two different types of molecular assemblies sustained by hydrogen bonds. Formation of the 1:1 salts was expected for **pipe**, **A12C4**, **BA15C5**, and **A18C6**, whereas **teta** and **DA18C6**, with four and two NH-groups, respectively, were expected to form 1:2 salts. In this study we also analyze the crystal packing in these new structures with an emphasis on the general features that could be more broadly relevant in the context of crystal design.

Experimental Section

All chemicals were of analytical grade and were used without further purification. Salts were obtained by mixing of equimolar amounts of the corresponding macrocycle and **saH** (or acetylsalicylic acid) dissolved in a water/methanol solution. Suitable microanalyses for C, H, and N were obtained for all compounds using a Perkin-Elmer 240 C device.

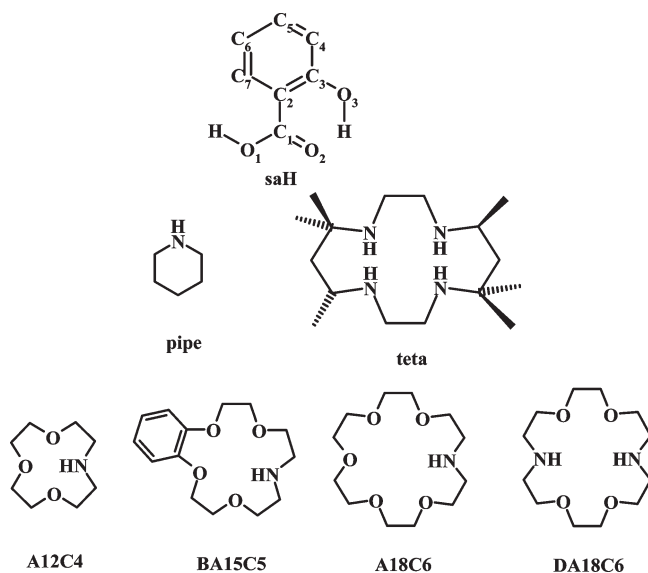
Salicylic Acid with Piperidine, [pipeH][sa]. Piperidine (85 mg, 1 mmol) and salicylic acid (138 mg, 1 mmol) were dissolved in methanol (25 mL) at 64 °C and then allowed to evaporate at room temperature. The yield of crystalline solid was close to quantitative. Transparent colorless crystals, soluble in methanol, ethanol, acetone, mp 108–110 °C. Found (%): C, 64.51; H, 7.72; N, 6.29. Required for $C_{12}H_{17}NO_3$ (%): C, 64.55; H, 7.67; N, 6.27.

Salicylic Acid with meso-5,7,7,12,12,14-Hexamethyl-1,4,8,11-tetraazacyclotetradecane, [tetaH₂][sa]₂. *meso*-5,7,7,12,12,14-Hexamethyl-1,4,8,11-tetraazacyclotetradecane (142 mg, 0.5 mmol) and salicylic acid (138 mg, 1 mmol) were dissolved in water–methanol (3 mL/10 mL) at 64 °C and allowed to slowly evaporate at room temperature. Transparent colorless crystals, soluble in methanol, ethanol, acetone, mp ≥280–282 °C (dec.). Found (%): C, 64.31; H, 8.60; N, 9.94. Required for $C_{30}H_{48}N_4O_6$: C, 64.26; H, 8.63; N, 9.99.

Salicylic Acid with 1,4,7-Trioxa-10-azacyclododecane, [A12C4H][sa]. 1,4,7-Trioxa-10-azacyclododecane (175 mg, 1 mmol) and salicylic acid (138 mg, 1 mmol) were dissolved in water/methanol (0.5 mL/5 mL) at 64 °C and allowed to slowly evaporate at room temperature. The resulting solid was recrystallized from acetone/hexane (5 mL/5 mL). Transparent colorless crystals, soluble in methanol, ethanol, acetone, mp 166–167 °C (dec.). Found (%): C, 57.54; H, 7.42; N, 4.43. Required for $C_{15}H_{23}NO_6$ (%): C, 57.50; H, 7.40; N, 4.47.

Salicylic Acid with 2,3,6,7,8,9,11,12-Octahydro-5*H*-1,4,10,13,7-benzotetraoxazacyclopentadecine, [BA15C5H][sa]. 2,3,6,7,8,9,11,12-Octahydro-5*H*-1,4,10,13,7-benzotetraoxaza-cyclopentadecine (134 mg, 0.5 mmol) and salicylic acid (69 mg, 0.5 mmol) were dissolved in water/methanol (1 mL/10 mL) at 64 °C and allowed to slowly evaporate at room temperature. Colorless, transparent crystals, soluble in methanol, ethanol, acetone, mp 140–141 °C. (dec.). Found (%): C, 62.20; H, 6.75; N, 3.47. Required for $C_{21}H_{27}NO_7$ (%): C, 62.21; H, 6.71; N, 3.45.

Scheme 1. Target Salicylic Acid with the Numbering Scheme, and Cyclic Aza-Molecules



Salicylic Acid with 1,4,7,10,13-Pentaoxa-16-azacyclooctadecane, [A18C6H]₂[sa]·2H₂O. 1,4,7,10,13-Pentaoxa-16-azacyclooctadecane (263 mg, 1 mmol) and salicylic acid (138 mg, 1 mmol) were dissolved in water/methanol (0.5 mL/5 mL) at 64 °C and allowed to slowly evaporate at room temperature. To obtain single crystals, the resulting solid was recrystallized from acetone and hexane (5 mL/5 mL). Transparent colorless crystals, soluble in methanol, ethanol, acetone, mp 83–85 °C (dec.). Found (%): C, 52.13; H, 8.09; N, 3.26. Required for $C_{19}H_{35}NO_{10}$ (%): C, 52.16; H, 8.06; N, 3.20.

Salicylic Acid with 1,4,10,13-Tetraoxa-7,16-diazacyclooctadecane, [DA18C6H₂]₂[sa]₂·3H₂O. 1,4,10,13-Tetraoxa-7,16-diazacyclooctadecane (132 mg, 0.5 mmol) and (69 mg, 0.5 mmol) salicylic acid were dissolved in water/methanol (1 mL/10 mL) at 64 °C and allowed to slowly evaporate at room temperature. Transparent colorless crystals, soluble in methanol, ethanol, acetone, mp 156–157 °C (dec.). Found (%): C, 51.22; H, 8.33; N, 6.24. Required for $C_{28}H_{44}N_4O_6S_4$: C, 50.87; H, 6.71; N, 8.48; S, 19.41.

Single-Crystal X-ray Data Collection and Structure Determinations. X-ray data for all complexes were collected on a Bruker SMART-APEX CCD diffractometer using graphite-monochromated Mo K α radiation at 100 K. There was no intensity decay. Structure solutions were performed by direct methods (SHELXS-97) and refined by full-matrix least-squares methods on F^2 (SHELXL-97).⁶³ In all but [DA18C6H₂]₂[sa]₂·3H₂O, non-hydrogen atoms were refined anisotropically. In [pipeH][sa], all H-atoms were localized *via* the inspection of a difference Fourier map and refined freely. In all the other structures, H-atoms attached to carbons were included in idealized positions using a riding model with isotropic temperature factors 1.2 times that of the parent carbon atom, whereas those on N and O(water) atoms were found from difference Fourier maps and refined in an isotropic approximation, except for the case of [DA18C6H₂]₂[sa]₂·3H₂O, where such H atoms were not located. In [A12C4H][sa], the hydroxyl group in the sa unit A is disordered with H atoms in the other *o*-position, and it was refined with occupancies of 0.55 and 0.45, respectively. The crystal structure of [DA18C6H₂]₂[sa]₂·3H₂O was solved and refined in the centrosymmetric space group *P*1. It is comprised of two similar but crystallographically independent complexes. In both complexes the crown ether molecule resides on the crystallographic inversion center, while both sa anions and water molecules occupy general positions and are disordered over two positions with equal occupancies. Analysis of the disordered positions and intermolecular contacts unambiguously showed that although each crown molecule resides on the inversion center, it has a different-face environment, and each complex is noncentrosymmetric. The observed centrosymmetric structure is the result of superposition in the crystal of two generally noncentrosymmetric structures. Nevertheless, attempts to solve this structure in the noncentrosymmetric

space group *P*1 did not change the disordering pattern for **sa** and water molecules and did not show any deviation in the geometrical parameters of the macrocyclic molecule compared with that in the centrosymmetric space group. The **sa** anions were refined isotropically using a rigid group approximation. The N-bound H-atoms were included in idealized positions in a riding model with isotropic temperature factors 1.2 times the parent nitrogen atom temperature factor. The disordered water molecule O1W was refined with the partial occupancy of 0.71. The poor crystal quality for compound [DA18C6H₂][sa]₂·3H₂O did not permit reliable placement of the H-atoms of the water molecules. Crystallographic data for structures reported in this paper have been deposited with the Cambridge Crystallographic Data Centre as supplementary publication CCDC Nos. 779399–779404. Copies of these data can be obtained free of charge via <http://www.ccdc.cam.ac.uk/conts/retrieving.html> or from the Director, CCDC, 12 Union Road, Cambridge CB2 IEZ, U.K.; fax (+44) 1223-336-033; or e-mail deposit@ccdc.cam.ac.uk. The structure graphics shown in the figures were created using the Mercury software package version 2.3.⁶⁴ The Packing Index (PI) was calculated with the program PLATON.⁶⁵ Crystal data together with further details of the data collections and refinement are given in Table 2.

Results and Discussion

In two parallel series of supramolecular syntheses, we used as API acetylsalicylic acid (aspirin) or salicylic acid (**saH**) and as a cocrystallization partner the aza cycles piperidine and *meso*-5,7,7,12,12,14-hexamethyl-1,4,8,11-tetraazacyclotetradecane, the aza-crown ethers A12C4, BA15C5, A18C6, and DA18C6, the crown ether 18C6, and *cis*-*syn*-*cis*- and *cis*-*anti*-*cis*-stereoisomers of dicyclohexyl-18C6. All reactions were carried out under similar synthetic conditions, by mixing of equimolar amounts of water/methanol solutions of **saH** or aspirin and a corresponding cyclic molecule. The crystalline products were obtained only for *N*-bases, and their X-ray structural analyses indicated that in the reactions with aspirin, due to its hydrolysis, the final products represented complexes of **saH** identical to those obtained starting from **saH**. The crystal structures of six new compounds were determined by a single-crystal X-ray method. The carbon–oxygen bond distances in the carboxylic group in all structures were consistent with the deprotonated form (the C–O distances range within 1.240–1.278 Å, Table 3). In addition, the Fourier difference maps revealed that the acidic protons are positioned in proximity to the *N*-atom of the cyclic molecule, and the compounds were classified as proton-transfer complexes or salts. Hydrogen bond parameters are listed in Table 4. The hydroxy group of **saH** is involved in an intramolecular O–H(hydroxy)···O(carboxy) hydrogen bond with the carboxylic group to form a *S*₁(6) ring, inherent in other 2-hydroxybenzoic and 2-hydroxynaphthoic acids.^{9,12}

[**PipeH**][**sa**] crystallizes in the monoclinic *P*2₁/c space group. The asymmetric unit consists of one piperidinium cation and one **sa** anion. Two cations and two anions form a centrosymmetric assembly, giving rise to the *R*₄⁴(12) heterosynthon. The N(1)···O(1) (2 – *x*, 1 – *y*, 1 – *z*) and N(1)···O(2) distances are equal to 2.721(1) and 2.771(1) Å, respectively (Figure 1a, Table 4). The mean plane of the piperidinium cation, which adopts a chair conformation, and the planar **sa** anion are inclined at a shallow angle of 39.4°. Separated by the piperidinium cations, two **sa** anions are at the O···O distance of 4.56 Å, measured across an inversion center of the heterotetramer. The heterotetramers are further combined into a 2D layer parallel to the *bc* plane by a C–H(**PipeH**)···O(3)(**sa**) hydrogen bond (C···O = 3.287 Å, H···O = 2.39 Å, ∠CHO = 156°) which involves an oxygen lone pair of the 2-hydroxy group. Thus, the layer is built of alternative four- and eight-membered H-bonded cycles. The **sa** anions related by the glide

Table 2. Summary of Crystal Data and Structure Refinement Parameters for Studied Compounds

compound	[pipeH][sa] ₂	[Al ₂ C ₄ H][sa]	[Al ₁₅ C ₅ H][sa]	[Al ₁₈ C ₆ H][sa]·2H ₂ O
formula	C ₁₂ H ₁₇ NO ₃ (C ₅ H ₁₂ N)(C ₇ H ₅ O ₃)	C ₃₀ H ₄₈ N ₂ O ₆ (C ₁₆ H ₃₈ N ₄)(C ₇ H ₅ O ₃) ₂	C ₂₁ H ₂₇ NO ₇ (C ₁₄ H ₂₂ NO ₄)(C ₇ H ₅ O ₃)	C ₁₉ H ₅ NO ₁₀ (C ₁₂ H ₂₈ N ₂ O ₄)(C ₇ H ₅ O ₃)·3H ₂ O
composition				
formula weight	223.27	560.72	640.76	592.63
crystal system	monoclinic	monoclinic	triclinic	triclinic
space group	<i>P</i> 2 ₁ /c	<i>P</i> 2 ₁ /c	<i>P</i> 1	<i>P</i> 1
<i>a</i> /Å	6.981(96)	7.7185(7)	5.4184(5)	9.434(2)
<i>b</i> /Å	18.7029(16)	18.8796(17)	12.6000(12)	12.5873(3)
<i>c</i> /Å	9.6814(8)	10.3126(9)	15.9635(16)	13.843(2)
α, deg	90	90.0	90	98.175(4)
β, deg	109.574(2)	92.642(2)	95.915(2)	90.721(2)
γ, deg	90	90	91.267(2)	111.355(3)
<i>V</i> /Å ³	1191.16(17)	1501.2(2)	997.14(17)	1511.7(6)
<i>Z</i>	4	2	8	2
<i>D</i> _c (mg m ⁻³)	1.245	1.240	1.354	1.321
<i>μ</i> (Mo K α)/mm ⁻¹	0.089	0.086	0.105	0.104
<i>F</i> (000)	480	608	1344	944
reflections collected/	21388/2732	9064/3263	17347/6003	6186/4237
unique reflections with <i>I</i> > 2σ(<i>I</i>)	1.004	1.048	[<i>R</i> (int) = 0.0664]	[<i>R</i> (int) = 0.0698]
goodness of fit reflections with <i>I</i> > 2σ(<i>I</i>)	2427	2722	0.970	0.958
<i>R</i> , w <i>R</i> [<i>I</i> > 2σ(<i>I</i>)]	0.0388, 0.1060	0.0512, 0.1400	0.0494, 0.1226	0.0377, 0.0623
			3232	3232
			0.0518, 0.0912	0.0923, 0.2341

Table 3. Selected Parameters for Studied Compounds

parameter	[pipeH][sa]	[tetaH ₂][sa] ₂	[A12C4H][sa]	[BA15C5H][sa]	[A18C6H][sa]·2H ₂ O	[DA18C6H ₂][sa] ₂ ·3H ₂ O
base/sa/H ₂ O ratio	1:1	1:2	1:1	1:1	1:1.2	1:2.3
melting point/°C	108–110	280–282	166–167	140–141	83–85	156–157
O—C/A	1.249(1) 1.278(1)	1.240(2) 1.290(2)	1.258(4) 1.268(4) 1.258(3) 1.272(3)	1.264(2) 1.265(2)	1.250(3) 1.272(3)	1.266
base ^b /sa angle/deg	39.4	70.5	68.8 69.2	89.1	43.9	80.3 86.5 79.4 82.5
sa/sa angle/deg	60.9	84.1	84.8	89.1	67.7	82.5(M/P) 86.5(N/R)
Cg(sa)···Cg(sa)/Å	6.25	5.28	5.19 5.29	5.10	5.22	5.31–5.71
PI/%	67.7	69.4	71.5	70.7	70.7	^a

^a Packing index is not available—disordered structure. ^b Base plane is calculated through the cyclic heteroatoms, for pipeH—through all non-H atoms.

Table 4. Hydrogen Bonds (Å and deg) for Studied Compounds^a

D—H···A	d(D—H)	d(H···A)	d(D···A)	∠(DHA)
[pipeH][sa]				
O(3)—H(1O3)···O(2)	1.02(2)	1.54(2)	2.504(1)	155(2)
N(1)—H(1N)···O(2)	0.93(2)	1.79(2)	2.721(1)	172(1)
N(1)—H(2N)···O(1) ⁱ	0.90(2)	1.87(2)	2.771(1)	179(1)
[tetaH₂][sa]₂				
O(3)—H(1O3)···O(2)	1.11(2)	1.45(2)	2.511(1)	156(2)
N(1)—H(1)···O(2) ⁱ	1.01(2)	1.69(2)	2.701(2)	177(2)
N(1)—H(2)···N(2)	1.00(2)	1.94(2)	2.775(2)	140(2)
N(2)—H(3)···O(1) ⁱ	0.87(2)	2.25(2)	3.095(2)	162(1)
[A12C4H][sa]				
O(3A)—H(3A)···O(2A)	1.08(5)	1.48(5)	2.451(4)	146(4)
O(3AA)—H(3AA)···O(1A)	1.07(5)	1.45(5)	2.490(6)	162(6)
N(1A)—H(1)···O(5A)	0.82(3)	2.09(3)	2.827(3)	148(3)
N(1A)—H(2)···O(2A)	1.02(3)	1.65(3)	2.655(3)	168(2)
C(14A)—H(14A)···O(1A)	0.99	2.46	3.356(4)	150
O(3B)—H(3B)···O(2B)	1.01(3)	1.59(3)	2.516(3)	150(3)
N(1B)—H(3)···O(5B)	0.90(3)	2.07(3)	2.842(4)	143(3)
N(1B)—H(4)···O(1B)	1.08(3)	1.56(4)	2.635(3)	171(3)
C(14B)—H(14D)···O(2B)	0.99	2.47	3.382(4)	153
[BA15C5H][sa]				
O(3)—H(1O3)···O(2)	0.95(2)	1.63(2)	2.528(2)	157(2)
N(1)—H(1)···O(1)	0.99(2)	1.64(2)	2.626(2)	172(2)
[A18C6H][sa]·2H₂O				
O(3)—H(1O3)···O(2)	1.00(2)	1.50(2)	2.473(2)	163(2)
N(1)—H(1)···O(1)	0.99(3)	1.80(3)	2.775(2)	166(2)
N(1)—H(2)···O(1W)	0.97(2)	1.81(3)	2.779(2)	171(2)
O(1W)—H(1W1)···O(7)	0.80(2)	2.19(2)	2.992(2)	174(2)
O(1W)—H(2W1)···O(5)	0.81(2)	2.11(2)	2.920(2)	175(2)
O(2W)—H(1W2)···O(1W) ⁱⁱ	0.77(3)	2.17(3)	2.901(2)	159(3)
O(2W)—H(2W2)···O(1)	1.03(4)	1.89(5)	2.918(2)	172(4)
C(9)—H(9B)···O(2)	0.99	2.46	3.413(3)	162
[DA18C6H₂][sa]₂·3H₂O				
N(4A)—H(4A1)···O(1W)	0.92	1.94	2.853(8)	173
N(4A)—H(4A1)···O(1W')	0.92	2.12	2.84(4)	134
N(4A)—H(4A2)···O(2N) ⁱⁱ	0.92	1.90	2.78(2)	157
N(4A)—H(4A2)···O(1M) ⁱⁱ	0.92	1.90	2.772(7)	157
N(4A)—H(4A2)···O(2M) ⁱⁱ	0.92	2.22	2.938(2)	134
N(4B)—H(4B1)···O(2W)	0.92	1.77	2.687(1)	171
N(4B)—H(4B1)···O(2W')	0.92	2.21	2.964(9)	138
N(4B)—H(4B2)···O(1P) ⁱⁱⁱ	0.92	1.77	2.666(7)	165
N(4B)—H(4B2)···O(2R) ⁱⁱⁱ	0.92	2.06	2.91(1)	151
O(3M)—H(3M)···O(2M)	0.84	1.80	2.544	146
O(3N)—H(3N)···O(2N)	0.84	1.80	2.544	146
O(3P)—H(3P)···O(2P)	0.84	1.80	2.544	146
O(3R)—H(3R)···O(2R)	0.84	1.80	2.544	146

^a Symmetry transformation for acceptor: (i) $2 - x, 1 - y, 1 - z$; (ii) $1 - x, 1 - y, 1 - z$; (iii) $1 - x, 1 - y, -z$.

plane are arranged with an *m/p* edge of one ring directed to the ring face of the adjacent anion, and they form the dihedral angle

of 60.9°, with the distance between the centroids of the aromatic rings being equal to 6.25 Å. The layer thickness corresponds to the shortest *a* axis (Figure 1c). Adjacent layers are held together by van der Waals forces. The crystal density of 1.245 g cm⁻³ and the packing coefficient (67.7%) of [pipeH][sa] are significantly smaller than those for salicylic acid itself (1.468 g cm⁻³, 72.0%) and for the relative compounds discussed in ref 10.

[TetaH₂][sa]₂. The anticipated hydrogen-bonded trimer [sa][tetaH₂][sa] resides around a crystallographic center of symmetry in the monoclinic crystal, having space group P2₁/c (Figure 2a). The tetraazacycle comprises four amino groups and generally captures two protons from acidic species to form a dication [tetaH₂]²⁺. The dication conformation is folded by two intramolecular NH···N hydrogen bonds, N(1)···N(2) = 2.775(2) Å (Table 4). In the formula unit, two sa anions act in a chelate mode across the macrocyclic cavity, giving rise to two R₃³(8) rings, each including two intermolecular NH···O hydrogen bonds of 2.701(2) and 3.095(2) Å and one above-mentioned intramolecular hydrogen bond. The similar modes of the cycle protonation, and complex organization were registered in other complexes of teta with aromatic acids.^{4,66} The sa anion forms the dihedral angle of 70.5° with the mean plane of the N₄-cyclic atoms. Although the O···O expansion between the related by the center of inversion sa anions across the cycle increases up to 6.83 Å, the general packing motif bears close resemblance to [pipeH][sa]. The translated along *c* direction complexes are linked by weak C—H···O hydrogen bonds involving the 2-hydroxy group (C···O = 3.474, H···O = 2.57 Å, ∠CHO = 153°) to form a ribbon (Figure 2b). The edge-to-face arrangement of the sa anions across the ribbons is characterized by the dihedral angle 84.08° and the centroid-to-centroid distance 5.28 Å, with the *m/p*-edge pointing toward the neighboring sa anion. Similar to the case of [pipeH][sa], the layers pack along the shortest *a* axis, and the thickness of the layer increases (Figure 2c, Table 2). The PI increases up to 69.4%.

[A12C4H][sa] crystallizes in the monoclinic P2₁/c space group. The asymmetric unit contains two sa anions (A and B) and two cyclic cations (A and B) (Figure 3a and b). The conformation of the both cycles is folded by the intramolecular N(1)···O(5) hydrogen bond (Table 4). The hydroxyl group in the sa unit A is disordered with the H atom in another *o*-position, while the positions for all other atoms of the anion coincide.

The sa—cycle interactions occur in a chelate mode via strong NH···O hydrogen bonds, N(1A)···O(2A) = 2.655(3) Å and N(1B)···O(1B) = 2.635(3) Å, and weak CH···O

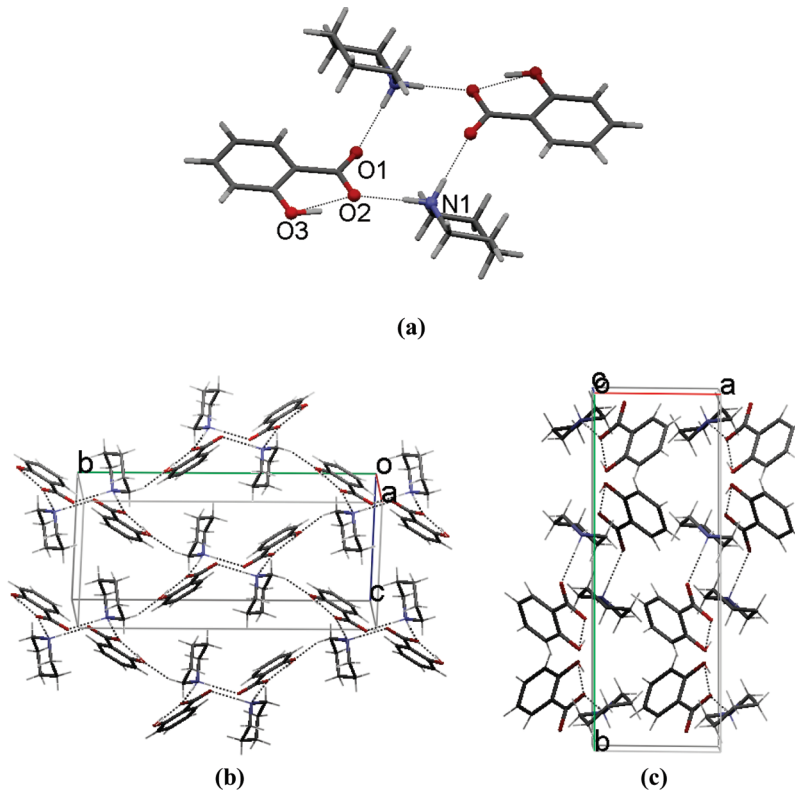


Figure 1. Perspective views for [pipeH][sa]: (a) four-component complexes defined by the $R_4^4(12)$ hydrogen-bond pattern; (b) H-bonded layer sustained by the combination of $NH \cdots O$ and $CH \cdots O$ interactions; (c) packing of the layers.

hydrogen bonds, $C(14A) \cdots O(1A) = 3.356(4) \text{ \AA}$ and $C(14B) \cdots O(2B) = 3.382(4) \text{ \AA}$, giving rise to the $R_2^2(8)$ hydrogen-bonding nonplanar pattern for two (A and B) formula units. The same mode of interaction was registered in the salt of *p*-aminobenzoic acid with **A12C4**.⁴ The A and B complexes are associated into chains *via* weak $CH(\text{cycle}) \cdots O(\text{cycle})$ interactions. The chains related by the translation a pack to form the edge-to-face interactions giving rise to the herringbone arrangement of the **sa**(A)/**sa**(B) dihedral angle of 84.83° and by centroid-to-centroid distances of 5.19 \AA and 5.29 \AA for A/B and B/A pairs, respectively (Figure 3c). The *p*-H atom of **sa**(B) pointed toward the hydroxyl group of the adjacent **sa**(A) anion, $C(5B) \cdots O(3A) = 3.741$, $H \cdots O = 2.80 \text{ \AA}$, while the *m/p* edge of **sa**(A) is above the translated B anion. The **sa** anions are completely buried within the layers parallel to the *ac* plane, whose thickness is defined by the **A12C4H** cations (Figure 3d). PI adopts the value of 71.5%.

[**BA15C5H**][sa] crystallizes in the triclinic $P\bar{1}$ space group. In the asymmetric unit there are one macrocyclic cation and one **sa** anion linked by the single $NH \cdots O$ hydrogen bond, $N(1) \cdots O(1) = 2.626(2) \text{ \AA}$. The second oxygen atom of the carboxylic group O(2) does not participate in any short intermolecular contacts (Figure 4a). Although the second H-atom of the azonia-group is pointed inside the macrocyclic cavity, all $N(1) \cdots O(\text{cycle})$ distances exceed the range of the hydrogen-bonded contacts. The complexes stack along the shortest *a* direction (Figure 4b, Table 2). The stacks related by the center of symmetry are packed in a way to form the edge-to-face interactions between the **sa** anions and the aromatic rings of the macrocyclic cations, providing the dihedral angle between the aromatic units of 89.1° and the shortest centroid-to-centroid distance

of 5.10 \AA . The crystal structure reveals a crystal packing with PI being 70.7% (Figure 4c).

[**A18C6H**][sa]·2H₂O crystallizes in the orthorhombic *Pca*₂ space group. The asymmetric unit is comprised of one macrocyclic cation, one **sa** anion, and two water molecules (Figure 5a). The charged units interact *via* a couple of hydrogen bonds, with $N(1) \cdots O(1) = 2.775(2)$ and $C(9) \cdots O(2) = 3.413(3) \text{ \AA}$ acting in a chelate mode identical to that one registered in the [**A12C4H**][sa], which in Etter's graph set notation can be described as the $R_2^2(8)$ pattern. The **sa** anion is inclined at an angle of 43.9° to the NO₅-macrocycle plane. Two water molecules fulfill different structural functions: water molecule O(1W) centers the macrocyclic cavity and acts as a double H-bond donor and a single H-bond acceptor, giving rise to three hydrogen bonds, and additionally links the O2W water molecule as an H-acceptor (Table 4). The second water molecule O2W, acting as a double H-bond donor, bridges the complexes into a chain along the *c* axis (Figure 5b). The related by the screw axis chains are packed in a zipper-like mode with the partial mutual interdigitation of the macrocycles and with the herringbone edge-to-face arrangement of the **sa** anions being described by the dihedral angle of 67.73° and the centroid-to-centroid distance of 5.22 \AA (Figure 5c). The PI of 70.7% is the same as that for [**BA15C5H**][sa].

[**DA18C6H**₂][sa]₂·3H₂O crystallizes in the triclinic space group $P\bar{1}$. The crystal is built of two quite similar but crystallographically independent complexes [**sa** M][cycle A]-[**sa** N]·2H₂O and [**sa** P][cycle B][**sa** R]·2H₂O. The poor crystal quality does not permit us to locate hydrogen atoms of water molecules and thus discuss the details of hydrogen bonding. Although the macrocyclic dication lies about an inversion center in the given structural model, it has a

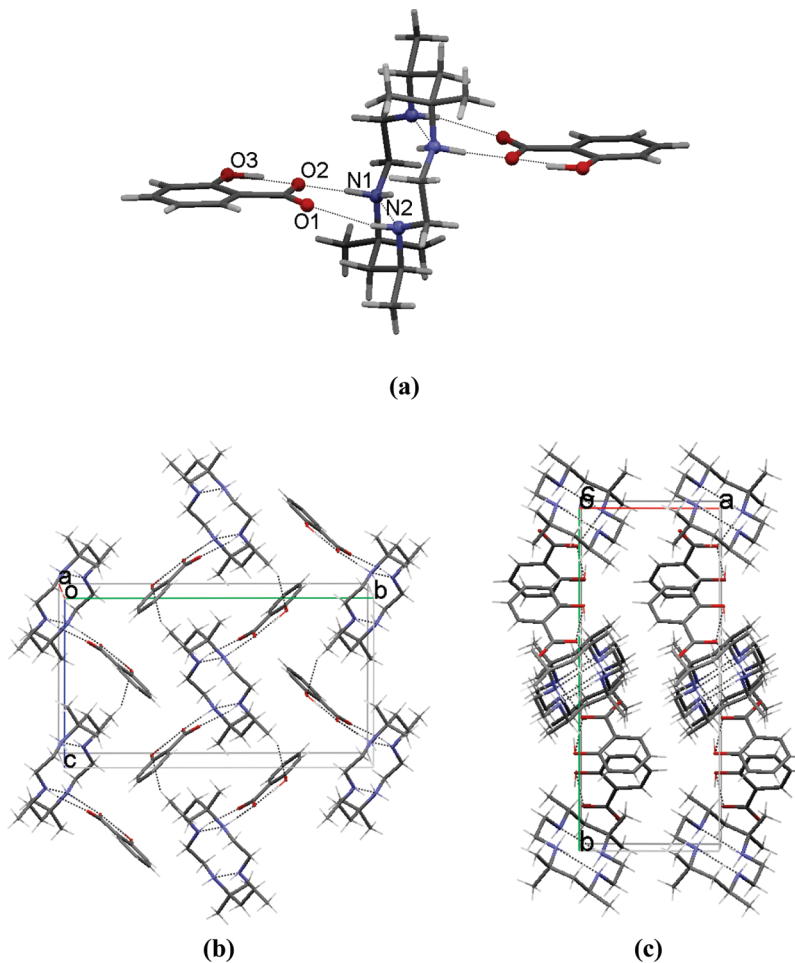


Figure 2. Perspective views for **[tetraH₂][sa]₂**: (a) three-component complex defined by the $R_3^3(8)R_2^2(10)R_3^3(8)$ succession; (b) the layer sustained by the combination of $NH \cdots O$, $CH \cdots O$, and $\pi - \pi$ edge-to-face interactions; (c) packing of the layers.

different-face environment (see details in the Experimental Section, Figure 6a, and Table 4). At one side of the crown ether the **sa** anion is linked with the macrocycle *via* a $NH \cdots O(\text{sa})$ hydrogen bond, while another oxygen atom of the carboxylate group interacts with the O1W water molecule being in a “perching” position which mediates the macrocyclic cation and **sa** anion *via* short $NH \cdots O(\text{water})$, $O(\text{cycle}) \cdots O(\text{water})$, and $O(\text{water}) \cdots O(\text{sa})$ contacts. Another side of the macrocycle is also occupied by the water molecule O3W, which again mediates the **sa** anion and macrocycle, although being in a “side position”. At this side, the **sa** anion acts in a bidentate cyclic mode, being coordinated to the same N(4) atom giving rise to the $R_1^2(4)$ hydrogen-bonding pattern. In two complexes, the **sa** anions are arranged approximately perpendicular to the N_2O_4 -plane of the macrocyclic cation, with the corresponding dihedral angles being 80.3 and 86.45° for cycle A and 79.4 and 82.5° for cycle B, respectively. Water molecule O2W bridges the complexes in the chain running along the *c* axis (Figure 6b). The A and B cycles in the chain are inclined at an angle of 58.0° (defined as the dihedral angle between their N_2O_4 planes), which provides the arrangement of the adjacent **sa** anions close to being perpendicular (Figure 6b). The adjacent chains meet by their **sa** anions, which are arranged again in a herringbone motif with the dihedral angle between the aromatic rings of about 87° and with the centroid-to-centroid distances being in the range 5.31–5.71 Å (Figure 6c).

The examination of Table 1 and our results reveal that **saH** is readily cocrystallized with *N*-bases of aromatic and aliphatic nature. The cocrystals are predominantly formed *via* rearrangement of the $R_2^2(8)$ carboxylic acid homosynthon to the $R_2^2(8)$ carboxylic acid–amide (CSD refcodes DKPSAL10, SLCADC01, MOXWAY), $R_2^2(7)$ carboxylic acid–pyridine (SODDOF, ODOHEV, XOBCAT), or $R_2^2(8)$ carboxylic acid–amino–pyridine (GEYSAE) planar supramolecular heterosynthons sustained by two practically parallel hydrogen bonds. The proton transfer that follows the formation of salts is capable of either occurring within the robust $R_2^2(8)$ heterosynthon in the case of topological complementarity of the components (EDATOS, FIXTAI, LEWROU, LOLDIA, DENXAW, CIQBIO, MIFWUT, SLCADB10, WEPTIV, XAGFAM) or disrupting it in favor of higher-dimensional aggregates (HURNEN, NIMDIW). In the case of salt bridges (BAKYES, BUSNIM, HABVIP, HABVOV, KAFSEQ, LUDDUJ, NICSAL, WANTOU, YAVRAO, YORJOF), the hydrogen bond distances are shorter than those between neutral motifs, and even one charge-assisted hydrogen bond, as in NICSAL and in **[BA15C5H][sa]**, appears to be enough for a stable structure. The water molecule that is typically inserted between the charged species often violates the predicted route of cocrystallization⁶⁷ and complicates the structural motifs (FIXTAI, HABVIP, HABVOV, KAFSEQ, WANTOU). The salts under discussion demonstrate the diverse modes of **sa** interactions with the cyclic cations, being a bidentate-bridging

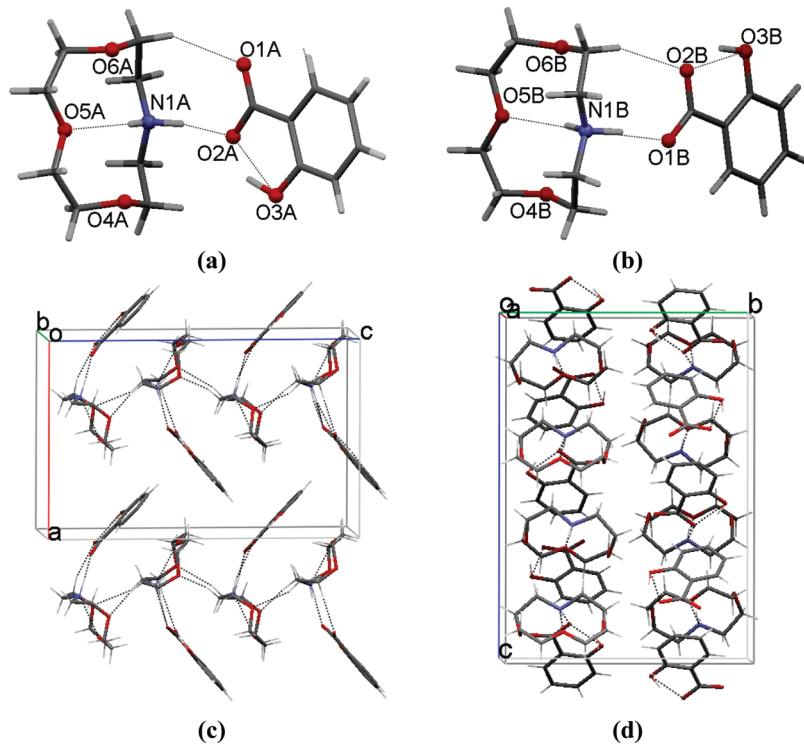


Figure 3. Perspective views for $[A12C4H][sa]$: (a and b) Two-component units defined by the $R_2^2(8)$ hydrogen-bond pattern. Only one position of the hydroxyl group is shown for the disordered **sa** (A) anion. (c) The layer sustained by the combination of $NH \cdots O$, $CH \cdots O$, and $\pi - \pi$ edge-to-face interactions. (d) Packing of the layers.

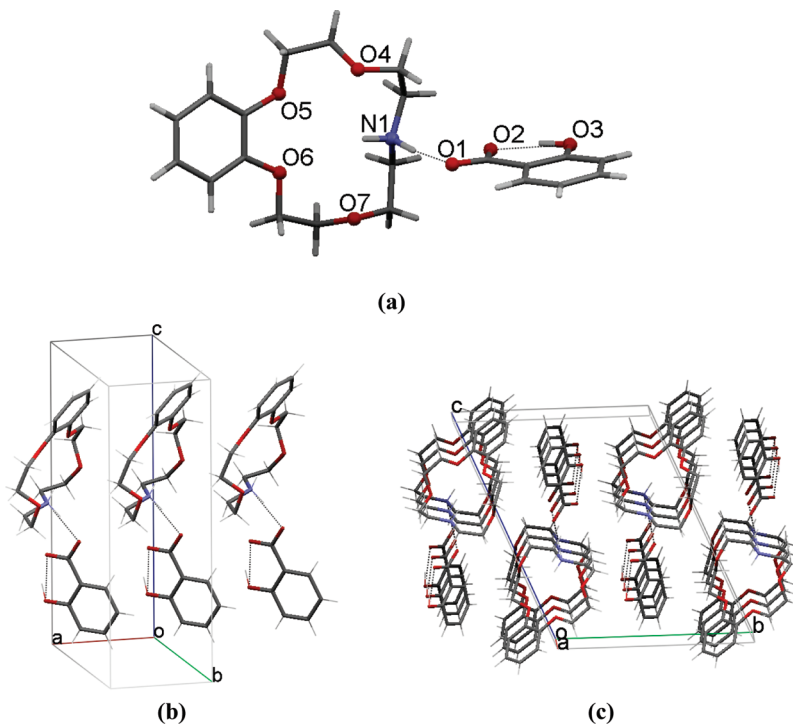


Figure 4. Perspective views for $[AB15C5H][sa]$: (a) two-component complex; (b) stack along the *a* direction; (c) crystal packing.

mode in **[pipeH][sa]** built on two strong charge-assisted $NH \cdots O$ hydrogen bonds, a chelate mode in **[tetraH₂][sa]₂** built again on a couple of strong $NH \cdots O$ hydrogen bonds or on a combination of strong $NH \cdots O$ and weak $CH \cdots O$ hydrogen bonds in **[A12C4H][sa]** and **[A18C6H][sa] · 2H₂O**, monodentate $NH \cdots O$ binding in **[BA15C5H][sa]**, and a combination of a

bidentate cyclic $R_1^2(4)$ hydrogen bonding pattern and a bidentate chelate mode in **[DA18C6H₂][sa]₂ · 3H₂O**.

In spite of the variety of **sa** · · · cyclic azonia cation interactions, all reported complexes invariably revealed at least one strong charge-assisted $NH \cdots O$ hydrogen bond. To estimate the reliability of such an intermolecular interaction,

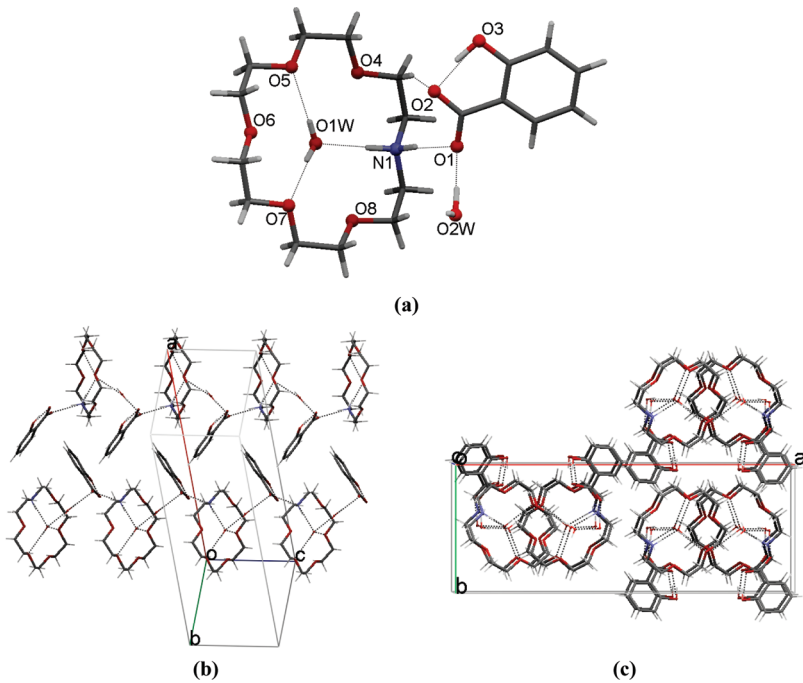


Figure 5. Perspective views for $[A18C6H][sa]\cdot 2H_2O$: (a) formula unit; (b) edge-to-face interactions between adjacent chains; (c) crystal packing.

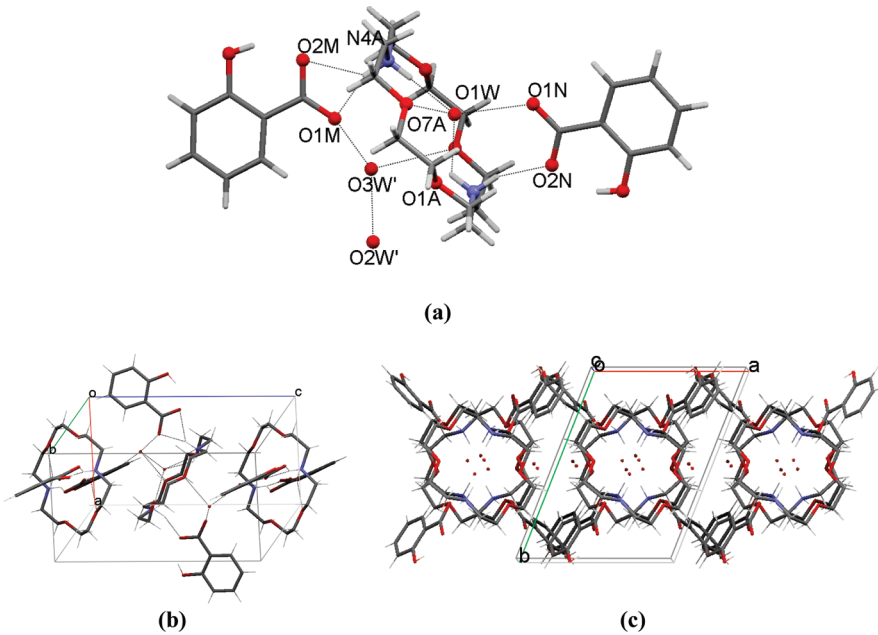
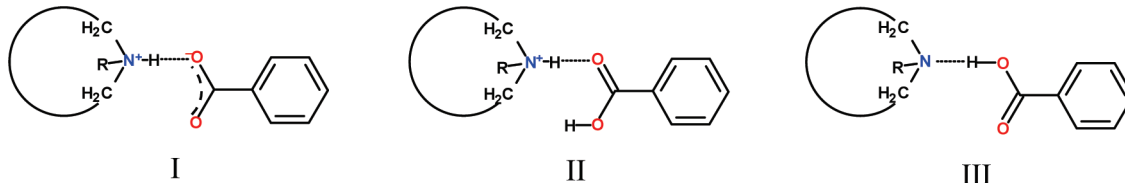


Figure 6. Perspective views for $(DA18C6H_2)(sa)_2\cdot 3H_2O$: (a) view of the complex defined by the macrocycle A; (b) hydrogen-bonding chain; (c) packing of the chains.

we have analyzed the CSD data (CSD v5.31, last update May 2010) involved in the search for the aromatic carboxylic acids and cyclic amines relative to the cyclic molecules reported herein in which the nitrogen atom in the sp^3 -hybridization state might form the H-bond. The searches were subjected to the following constraints: aromatic carboxylic group, either in neutral or deprotonated form, the cyclic N_{sp^3} -atom linked with at least two neighboring cyclic methylene groups, metal free structures, 3D coordinates present, repeated structures excluded. The survey of the CSD revealed 165 hits that obey our requirements. These entries include structures with obviously wrong assigned types of atoms (C or N atoms)

in the piperazinium moiety (KUFBIK, KUFBOD), disordered structures (EGODAF, NUKXOH), and structures where the N–H atom was not located (JIHCIM, PIPCBZ, PIPHBZ, WIFBUI, ZEJNAD). In the last case, the conclusion about the type of the $N\cdots O$ bond was originated from the analysis of the C–O distances in the carboxylic group. Of 165 hits, 132 (80%) exhibit a $NH^+\cdots O(COO^-)$ hydrogen bond (synthon I, Scheme 2); in five structures (3.0%), the positively charged azonia-group forms a H-bond with the neutral carboxylic group (synthon II), and six structures (3.6%) include the H-bonded interaction between the neutral components (synthon III). Thus, 143 (86.7%) hits revealed

Scheme 2. Supramolecular Heterosynthons Observed between the Aromatic Carboxylate Anion or Neutral Carboxylic Acid and a Cyclic Azonia or Amine Molecule: R = H, C



the intermolecular N \cdots O H-bonded interaction. Of 132 structures with a synthon I type of interaction, 61 represent hydrates; two hydrates were also observed in the structures with synthons II (WIZXIN, WOVWEJ) and III (MIPVIQ, SIXBAD), respectively. Only in one structure (FIFFIK) does the insertion of a water molecule destroy the robust NH $^+\cdots$ O(COO $^-$) synthon I. The lack of the charge-assisted hydrogen bonds in the majority of the remaining 22 structures (13.3%) is explained by the presence of the competing more acidic groups. This observation and our previous investigations (relevant to *p*-aminobenzoic and mefenamic acids)^{4,5} demonstrate the remarkable reliability of the N \cdots O interaction between the cyclic amines/azonia and aromatic carboxylates and the promising potential for design of multiple component crystals on the base of such interactions.

Along with the diverse types of **sa**–N-cycle interactions, the salts discussed herein demonstrate the different mutual arrangement of the components, which changes from the “side coordination” described by the shallow dihedral angle between the planes through the cyclic heteroatoms and planar skeleton of **sa** until the practically perpendicular arrangement. The corresponding dihedral angles are summarized in Table 3. In spite of the pronounced differences, the controlled by the H-bonds packing motifs reveal some common features, namely the similar arrangement of the **sa** anions, which preserve the herringbone edge-to-face packing pattern. Only in the case of [BA15C5H][sa], where the crown ether possesses its own aromatic moiety, is the **sa**/**sa** T-shaped arrangement substituted by the uniform **sa**/Ar-(crown) one, indicating that interactions between the aromatic units are still preserved. Thus, our results are in line with the conclusion made by Childs and co-workers for the carbamazepine containing structures²⁰ that interactions in the packing motif are cumulatively stronger than the hydrogen bonding motifs in the family of structures containing the same target molecule.

Conclusion

Six novel salts of salicylic acid with the azacycles piperidine and *meso*-5,7,7,12,12,14-hexamethyl-1,4,8,11-tetraazacyclotetradecane and the aza-crown ethers aza-12C4, benzoaza-15C5, aza-18C6, and diaza-18C6 were synthesized and characterized by single crystal X-ray diffraction analysis. All salts are sustained by the combination of charge-assisted and conventional hydrogen bonds. The Cambridge Structural Database search corroborates the reliability of the charge assisted hydrogen bonds, as the NH $^+\cdots$ O(COO $^-$) heterosynthon is formed in 80% of structures containing aromatic carboxylate and cyclic azonia functional groups, even in the presence of other hydrogen-bonding interactions. The edge-to-face arrangement of salicylate anions as the robust supramolecular motif is preserved in the crystals.

Supporting Information Available: X-ray crystallographic information in CIF format. This information is available free of charge via the Internet at <http://pubs.acs.org/>.

References

- (a) Nehm, S. J.; Rodríguez-Spong, B.; Rodríguez-Hornedo, N. *J. Cryst. Growth Des.* **2006**, *6*, 592–600. (b) Trask, A. V. *Mol. Pharmaceutics* **2007**, *4* (3), 301–309. (c) Stahl, P. H.; Wermuth, C. G. *Handbook of Pharmaceutical Salts: Properties, Selection, and Use*; Wiley-VCH/VHCA: Weinheim/Zurich, 2002. (d) Aakeroy, C. B. *Acta Crystallogr.* **1997**, *B53*, 569–586. (e) Maheshwari, C.; Jayasankar, A.; Khan, N. A.; Amidon, G. E.; Rodríguez-Hornedo, N. *J. CrystEngComm* **2009**, *11*, 493–500. (f) Shan, N.; Zaworotko, M. J. *Drug Discovery Today* **2008**, *13*, 440–446. (g) Lipinski, C. A.; Lombardo, F.; Dominy, B. W.; Feeney, P. J. *Adv. Drug Delivery Rev.* **1997**, *23*, 3–25. (h) Banks, W. A.; Kastin, A. J. *Brain Res. Bull.* **1985**, *15*, 287–292. (i) Begley, D. J. *J. Pharm. Pharmacol.* **1996**, *48*, 136–146. (j) Huang, L. F.; Tong, W. Q. *Adv. Drug Delivery Rev.* **2004**, *56*, 321–334. (k) Lednicer, D. *Strategies for Organic Drug Synthesis and Design*; Wiley: New York, 1998.
- (a) Andrews, G. P.; Zhai, H.; Tipping, S.; Jones, D. S. *J. Pharm. Sci.* **2009**, *98*, 4545–4556. (b) Fang, L.; Numajiri, S.; Kobayashi, D.; Ueda, H.; Nakayama, K.; Miyamae, H.; Morimoto, Y. *J. Pharm. Sci.* **2004**, *93*, 144–154. (c) Du, M.; Zhang, Z.-H.; Guo, W.; Fu, X.-J. *J. Cryst. Growth Des.* **2009**, *9*, 1655–1657. (d) Nichol, G. S.; Clegg, W. *J. Cryst. Growth Des.* **2009**, *9*, 1844–1850.
- (a) Remenar, J. F.; Morissette, S. L.; Peterson, M. L.; Moulton, B.; MacPhee, J. M.; Guzmán, H. R.; Almarsson, Ö. *J. Am. Chem. Soc.* **2003**, *125*, 8456–8457. (b) Childs, S. L.; Hardcastle, K. I. *J. Cryst. Growth Des.* **2007**, *7*, 1291–1304. (c) Childs, S. L.; Chyall, L. C.; Dunlap, J. T.; Smolenskaya, V. N.; Stahly, B. C.; Stahly, G. P. *J. Am. Chem. Soc.* **2004**, *126*, 13335–13342. (d) Schultheiss, N.; Lorimer, K.; Wolfe, S.; Desper, J. *J. CrystEngComm* **2010**, *12*, 742–749. (e) Orola, L.; Veidis, M. V. *J. CrystEngComm* **2009**, *11*, 415–417. (f) Bak, A.; Gore, A.; Yanez, E.; Stanton, M.; Tufekci, S.; Syed, R.; Akrami, A.; Rose, M.; Surapaneni, S.; Bostick, T.; King, A.; Neervannan, S.; Ostovic, D.; Koparkar, A. *J. Pharm. Sci.* **2008**, *97*, 3942–3956. (g) Viertelhaus, M.; Hilfiker, R.; Blatter, F. *J. Cryst. Growth Des.* **2009**, *9*, 2220–2228. (h) Stanton, M. K.; Bak, A. *J. Cryst. Growth Des.* **2008**, *8*, 3856.
- (a) Moulton, B.; Luisi, B. S.; Fonari, M. S.; Basok, S. S.; Ganin, E. V.; Kravtsov, V. Ch. *New J. Chem.* **2007**, *31*, 561–568.
- (a) Fonari, M. S.; Ganin, E. V.; Vologzhanina, A. V.; Antipin, M. Yu.; Kravtsov, V. Ch. *J. Cryst. Growth Des.* **2010**, *10*, 3647–3656.
- (a) Mackowiak, P. A. *Brief History of Antipyretic Therapy*. *Clin. Infect. Dis.* **2000**, *31* (Suppl 5), S154–6. (b) Wu, K. K. *Anti-Inflammatory Anti-Allergy Agents Med. Chem.* **2007**, *6*, 278–292.
- (a) Wheatley, P. *J. J. Chem. Soc.* **1964**, 6036–6048. (b) Vishweshwar, P.; McMahon, J. A.; Oliveira, M.; Peterson, M. L.; Zaworotko, M. J. *J. Am. Chem. Soc.* **2005**, *127*, 16802–16803. (c) Caira, M. R. *J. Crystallogr. Spectrosc. Res.* **1992**, *22*, 193–200. (d) Caira, M. R. *J. Chem. Crystallogr.* **1994**, *24*, 695–701. (e) Bond, A. D.; Boese, R.; Desiraju, G. R. *Angew. Chem., Int. Ed.* **2007**, *46*, 618–622.
- (a) Etter, M. C. *Acc. Chem. Res.* **1990**, *23*, 120–126.
- (a) Cochran, W. *Acta Crystallogr.* **1953**, *6*, 260–268. (b) Sundaralingam, M.; Jensen, L. H. *Acta Crystallogr.* **1965**, *18*, 1053–1058. (c) Bacon, G. E.; Jude, R. J. Z. *Kristallogr.* **1973**, *138*, 19–40. (d) Bolte, M. *Private Communication*, **2006**. (e) Munshi, P.; Row, T. N. G. *Acta Crystallogr.* **2006**, *B62*, 612–626.
- (a) Skovsgaard, S.; Bond, A. D. *J. CrystEngComm* **2009**, *11*, 444–453.
- (a) Lopez, C.; Claramunt, R. M.; Garcia, M. A.; Pinilla, E.; Torres, M. R.; Alkorta, I.; Elguero, J. *J. Cryst. Growth Des.* **2007**, *7*, 1176–1184.
- (a) Bucar, D.-K.; Henry, R. F.; Lou, X.; Duerst, R. W.; MacGillivray, L. R.; Zhang, G. G. Z. *J. Cryst. Growth Des.* **2009**, *9*, 1932–1943.

- (13) Berry, D. J.; Seaton, C. C.; Clegg, W.; Harrington, R. W.; Coles, S. J.; Horton, P. N.; Hursthouse, M. B.; Storey, R.; Jones, W.; Frisic, T.; Blagden, N. *Cryst. Growth Des.* **2008**, *8*, 1697–1712.
- (14) Bica, K.; Rogers, R. D. *ChemComm* **2010**, *46*, 1215–1217.
- (15) (a) Aakeröy, C. B.; Fasulo, M. E.; Desper, J. *Mol. Pharmaceutics* **2007**, *4*, 317–322. (b) Childs, S. L.; Stahly, G. P.; Park, A. *Mol. Pharmaceutics* **2007**, *4*, 323–338. (c) Hathwar, V. R.; Pal, R.; Guru Row, T. N. *Cryst. Growth Des.* **2010**, *10* (8), 3306–3310.
- (16) Haynes, D. A.; Jones, W.; Motherwell, W. D. S. *J. Pharm. Sci.* **2005**, *94*, 2111–2120.
- (17) Bruno, I. J.; Cole, J. C.; Edgington, P. R.; Kessler, M.; Macrae, C. F.; McCabe, P.; Pearson, J.; Taylor, R. *Acta Crystallogr.* **2002**, *B58*, 389–397.
- (18) Allen, F. N. *Acta Crystallogr.* **2002**, *B58*, 380–388.
- (19) Lu, E.; Rodriguez-Hornedo, N.; Suryanarayanan, R. *CrystEngComm* **2008**, *10*, 665–668.
- (20) Childs, S. L.; Wood, P. A.; Rodriguez-Hornedo, N.; Reddy, L. S.; Hardcastle, K. I. *Cryst. Growth Des.* **2009**, *9*, 1869–1888.
- (21) Klepeis, J.-H. P.; Evans, W. J.; Zaitseva, N.; Schwegler, E.; Teat, S. J. *Acta Crystallogr.* **2009**, *E65*, o2062.
- (22) Singh, T. P.; Vijayan, M. *Acta Crystallogr.* **1974**, *B30*, 557–562.
- (23) Wang, K.-W.; Pan, Y.-J.; Jin, Z.-M. *Z. Kristallogr.—New Cryst. Struct.* **2002**, *217*, 435–443.
- (24) Shimizu, N.; Nishigaki, S.; Nakai, Y.; Osaki, K. *Acta Crystallogr.* **1983**, *C39*, 891–893.
- (25) Shimizu, N.; Nishigaki, S.; Nakai, Y.; Osaki, K. *Acta Crystallogr.* **1984**, *C40*, 902.
- (26) Thanigaimani, K.; Muthiah, P. T.; Lynch, D. E. *Acta Crystallogr.* **2007**, *E63*, o4555–o4556.
- (27) Goswami, S.; Jana, S.; Hazra, A.; Fun, H.-K.; Anjum, S.; Atta-ur-Rahman *CrystEngComm* **2006**, *8*, 712–718.
- (28) Nishioka, F.; Nakanishi, I.; Fujiwara, T.; Tomita, K. *J. Inclusion Phenom. Macroyclic Chem.* **1984**, *2*, 701–714.
- (29) Varughese, K. I.; Kartha, G. *Acta Crystallogr.* **1982**, *B38*, 301–302.
- (30) Prabakaran, P.; Murugesan, S.; Muthiah, P. T.; Bocelli, G.; Righi, L. *Acta Crystallogr.* **2001**, *E57*, o933–o936.
- (31) Bartoszak-Adamska, E.; Dega-Szafran, Z.; Przedwojska, M.; Jaskolski, M. *Pol. J. Chem.* **2003**, *77*, 1711–1722.
- (32) Zhang, J.-N.; Shi, M.; Li, Q. *Chin. J. Struct. Chem.* **2005**, *24*, 151–158.
- (33) Patel, U.; Haridas, M.; Singh, T. P. *Acta Crystallogr.* **1988**, *C44*, 1264–1267.
- (34) Koh, L. L.; Xu, Y.; Gan, L. M.; Chew, C. H.; Lee, K. C. *Acta Crystallogr.* **1993**, *C49*, 1032–1035.
- (35) Smith, G.; Wermuth, U. D.; White, J. M. *CrystEngComm* **2003**, *5*, 58–61.
- (36) Byriel, K. A.; Gasperov, V.; Gloe, K.; Kennard, C. H. L.; Leong, A. J.; Lindoy, L. F.; Mahinay, M. S.; Pham, H. T.; Tasker, P. A.; Thorp, D.; Turner, P. *Dalton Trans.* **2003**, 3034–3040.
- (37) Lynch, D. E.; Smith, G.; Freney, D.; Byriel, K. A.; Kennard, C. H. L. *Aust. J. Chem.* **1994**, *47*, 1097–1115.
- (38) Byres, M.; Cox, P. J.; Kay, G.; Nixon, E. *CrystEngComm* **2009**, *11*, 135–142.
- (39) Flippin-Anderson, J. L.; Deschamps, J. R.; Brossi, A.; Greig, N. H. *Acta Crystallogr.* **2002**, *E58*, o853–o855.
- (40) Panneerelvam, P.; Stanley, N.; Muthiah, P. T. *Acta Crystallogr.* **2002**, *E58*, o180–o182.
- (41) Kim, H. S.; Jeffrey, G. A. *Acta Crystallogr.* **1971**, *B27*, 1123–1131.
- (42) Jebamony, J. R.; Muthiah, P. T. *Acta Crystallogr.* **1998**, *C54*, 539–540.
- (43) Limmatvapirat, S.; Yamaguchi, K.; Yonemochi, E.; Oguchi, T.; Yamamoto, K. *Acta Crystallogr.* **1997**, *C53*, 803–805.
- (44) Tamura, C.; Yoshikawa, M.; Sato, S.; Hata, T. *Chem. Lett.* **1973**, 1221–1224.
- (45) Gellert, R. W.; Hsu, I.-N. *J. Crystallogr. Spectrosc. Res.* **1983**, *13*, 99–105.
- (46) Gellert, R. W.; Hsu, I.-N. *Acta Crystallogr.* **1988**, *C44*, 311–313.
- (47) Oleksyn, B. J.; Serda, P. *Acta Crystallogr.* **1993**, *B49*, 530–534.
- (48) Muthiah, P. T.; Balasubramani, K.; Rytlewska, U.; Plutecka, A. *Acta Crystallogr.* **2006**, *C62*, o605–o607.
- (49) Fleck, M.; Tillmanns, E.; Haussuhl, S. *Z. Kristallogr.—New Cryst. Struct.* **2000**, *215*, 105–106.
- (50) McMahon, J. A.; Bis, J. A.; Vishweshwar, P.; Shattock, T. R.; McLaughlin, O. L.; Zaworotko, M. J. *Z. Kristallogr.* **2005**, *220*, 340–350.
- (51) Pertlik, F.; Mikenda, W.; Steinwender, E. *J. Crystallogr. Spectrosc. Res.* **1993**, *23*, 389–395.
- (52) Takata, N.; Shiraki, K.; Takano, R.; Hayashi, Y.; Terada, K. *Cryst. Growth Des.* **2008**, *8*, 3032–3037.
- (53) Du, L.; Zeng, W.; Liu, X.; Jian, F.-F. *Acta Crystallogr.* **2009**, *E65*, o1791.
- (54) Bartoszak-Adamska, E.; Dega-Szafran, Z.; Krociak, M.; Jaskolski, M.; Szafran, M. *J. Mol. Struct.* **2009**, *920*, 68–74.
- (55) Chitradevi, A.; Athimoolam, S.; Sridhar, B.; Asath Bahadur, S. *Acta Crystallogr.* **2009**, *E65*, o3041–o3042.
- (56) Reddy, L. S.; Bethune, S. J.; Kampf, J. W.; Rodriguez-Hornedo, N. *Cryst. Growth Des.* **2009**, *9*, 378–385.
- (57) Pedersen, C. J. *J. Am. Chem. Soc.* **1967**, *89*, 2495–2496.
- (58) (a) Simonov, Yu. A.; Fonari, M. S.; Lipkowski, J.; Ganin, E. V.; Yavolovskii, A. A.; Kamalov, G. L. *J. Struct. Chem.* **2009**, *50* (Suppl.1), S136–S142. (b) Fonari, M. S.; Furmanova, N. G.; Simonov, Yu. A. *J. Struct. Chem.* **2009**, *50* (Suppl.1), S124–S135. (c) Fonari, M. S.; Simonov, Yu. A.; Kravtsov, V. Ch.; Lipkowski, J.; Ganin, E. V.; Yavolovskii, A. A. *J. Mol. Struct.* **2003**, *647*, 129–140.
- (59) (a) Delgado, R.; Felix, V.; Lima, L. M. P.; Price, D. W. *Dalton Trans.* **2007**, 2734–2745. (b) Chen, T.; Wang, X.; He, Y.; Zhang, C.; Wu, Z.; Liao, K.; Wang, J.; Guo, Z. *Inorg. Chem.* **2009**, *48*, 5801–5809.
- (60) (a) Gokel, G. W.; Leevy, W. M.; Weber, M. E. *Chem. Rev.* **2004**, *104*, 2723–2750. (b) Kralj, M.; Tusek-Božić, L.; Frkanec, L. *Chem-MedChem* **2008**, *3*, 1478–1492. (c) Marjanović, M.; Kralj, M.; Supek, F.; Frkanec, L.; Piantanida, I.; Šmuc, T.; Tušek-Božić, L. *J. Med. Chem.* **2007**, *50*, 1007–1018.
- (61) ACD Lab Version 4.56/26; Advanced Chemical Development Inc.: Toronto, Canada, 2000.
- (62) Li, Z. J.; Abramov, Y.; Bordner, J.; Leonard, J.; Medek, A.; Trask, A. V. *J. Am. Chem. Soc.* **2006**, *128*, 8199–8210.
- (63) Sheldrick, G. M. *Acta Crystallogr.* **2008**, *A64*, 112–122.
- (64) Macrae, C. F.; Edgington, P. R.; McCabe, P.; Pidcock, E.; Shields, G. P.; Taylor, R.; Towler, M.; van de Streek, J. *J. Appl. Crystallogr.* **2006**, *39*, 453–457.
- (65) Spek, A. L. *J. Appl. Crystallogr.* **2003**, *36*, 7–13.
- (66) (a) Gregson, R. M.; Glidewell, C.; Ferguson, G.; Lough, A. J. *Acta Crystallogr.* **2000**, *B56*, 39–57. (b) Lough, A. J.; Gregson, R. M.; Ferguson, G.; Glidewell, C. *Acta Crystallogr.* **2000**, *B56*, 85–93. (c) MacLean, E. J.; Teat, S. J.; Farrell, D. M. M.; Ferguson, G.; Glidewell, C. *Acta Crystallogr.* **2002**, *C58*, o470–o473.
- (67) (a) Infantes, L.; Fabian, L.; Motherwell, W. D. S. *CrystEngComm* **2007**, *9*, 65–71. (b) Clarke, H. D.; Arora, K. K.; Bass, H.; Kavuru, P.; Ong, T. T.; Pujari, T.; Wojtas, L.; Zaworotko, M. J. *Cryst. Growth Des.* **2010**, *10*, 2152–2167.